Plant Soil (2019) 435:309–321
https://doi.org/10.1007/s11104-018-3895-z

REGULAR ARTICLE

Fire changes the spatial distribution and sources of soil organic carbon in a grassland-shrubland transition zone

**Guan Wang · Junran Li · Sujith Ravi ·
Bethany P. Theiling · Joel B. Sankey**

Received: 13 June 2018 / Accepted: 20 November 2018 / Published online: 1 December 2018

Abstract

Aims In many mixed grass-shrub ecosystems, increased shrub biomass tends to promote overall carbon storage, but the distribution of carbon pools may be complicated by disturbances such as wildfires. We investigated the spatial distribution of surface soil organic carbon (SOC) and its relative contribution from grasses and shrubs after fires in a grass-shrub transition zone in the northern Chihuahuan Desert, USA.

Methods We used a prescribed fire to create a burned treatment, then collected soil and plant samples. The biogeochemical approaches, geostatistical analyses, and carbon partitioning analyses were used to quantify the SOC and soil $\delta^{13}C$ spatial patterns.

Results Before the prescribed fire, up to 98% of the spatial dependence of SOC was autocorrelated at a distance of 1.91 m, corresponding to the approximate average shrub canopy diameter, but the spatial dependence dropped to 81% at a larger autocorrelation distance (3.74 m) two windy seasons after the fire. C_4 grasses and C_3 shrubs contributed approximately equal amounts of carbon to the surface SOC pool before the prescribed fire. However, C_4 grasses became the dominant source of SOC two windy seasons following the fire. For individual microsites, a substantially increased proportion of SOC was derived from C_4 grasses at the shrub microsites following the fire.

Conclusions The higher proportion of C_4 grasses-derived SOC at the shrub microsites post-fire suggests that SOC may have preferred pathways to move among different microsites following fire disturbance. The distinct spatial distribution patterns of $\delta^{13}C$, and the increased contribution of SOC from grasses may be explained by the rapid recovery of grasses following the fire. Overall, our results provide insights into how fire might be used as a management tool to alter soil carbon pools in the context of shrub encroachment.

Keywords Prescribed fire · Soil organic carbon · Soil $\delta^{13}C$ · Carbon source partitioning · Microsite

Abbreviations

SOC	Soil organic carbon

Introduction

Dryland soils represent an important global carbon (C) pool and store over a quarter of global soil organic

Responsible Editor: Lucas Silva.

G. Wang (✉) · J. Li · B. P. Theiling
Department of Geosciences, The University of Tulsa,
Tulsa, OK 74104, USA
e-mail: guw647@utulsa.edu

S. Ravi
Department of Earth and Environmental Science,
Temple University,
Philadelphia, PA 19122, USA

J. B. Sankey
US Geological Survey, Southwest Biological Science Center,
Grand Canyon Monitoring and Research Center,
Flagstaff, AZ 86001, USA

carbon (SOC) (Eswaran et al. 2000; Campbell et al. 2008; Sarukhan et al. 2005). Over the past 150 years, many arid and semiarid grasslands have been encroached by woody shrubs worldwide, and such an ecosystem change has been particularly well documented in the desert grasslands of the southwestern United States (Schlesinger et al. 1990; Jackson et al. 2002; D'Odorico et al. 2012). Shifting dominance among herbaceous and woody vegetation has important implications for local pastoral economics, biodiversity, nutrient and carbon distribution and storage, and human health (Jackson et al. 2002; Li et al. 2008, 2009a; Ravi et al. 2009; D'Odorico et al. 2012). Changes in C distribution and storage, in particular, are of vital importance to the maintenance of soil quality and productivity, and also affect the competition between grasses and shrubs (Plaza-Bonilla et al. 2015; Archer et al. 2017).

It is generally recognized that the invasion of woody vegetation into grasslands and savannas may increase the total C stored above- though not below-ground in those ecosystems (Jackson et al. 2002; Bird et al. 2002; Barger et al. 2011; Petrie et al. 2015). However, C storage dynamics may be additionally complicated by disturbances such as wildfire, which not only decreases above-ground C via combustion of plants, but can also alter the spatial distribution and concentration of C stored below-ground in soil (Sankey et al. 2012a, 2012b; Turnbull et al. 2012). Moreover, changes in the relative abundances of grasses and shrubs at different stages of shrub encroachment, or at different stages of recovery post-fire, may dynamically alter the contributions of plants to soil C storage in ways not fully understood in many environments. Owing to the potentially significant impacts of fire and vegetation changes to C storage during the process of woody shrub invasion, ecosystem-specific analyses of how prescribed fire changes the spatial distribution of SOC and alters the relative contribution of grasses and shrubs to SOC following fire are needed.

Biogeochemical approaches, especially stable isotopes, have been used to differentiate and trace different soil carbon sources in many ecosystems that hold shared dominance of two or more plant functional types (Bond et al. 1994; West et al. 2006; Bai et al. 2009; Wang et al. 2009; Puttock et al. 2014; Minckley et al. 2016). In the northern Chihuahuan Desert of the United States where our study is focused, two dominant vegetation types, grasses and shrubs, differ in their photosynthetic pathways. Shrubs utilize the C_3 photosynthetic pathway with typical $\delta^{13}C$, whereas grasses typically utilize the C_4 photosynthetic pathway (e.g., Bender 1968; Smith and Epstein 1971; Deines 1980). Because of the distinct $\delta^{13}C$ signatures for C_3 and C_4 plants, mixing models using $\delta^{13}C$ compositions of plants and soil provide a unique tool to quantify the contribution of C_3 and C_4 vegetation to total SOC (Farquhar et al. 1989; Wang et al. 2009).

Herein, we assessed the spatial distribution of SOC in a grass to shrub transition zone in the northern Chihuahuan Desert, United States, prior to and following a prescribed fire, and characterized the relative contributions of SOC from C_4 grasses and C_3 shrubs using stable carbon isotopes of soils and plants. Prescribed fire is used in this and other desert ecosystems as a management tool to maintain grassland communities that are threatened by degradation due to woody plants encroachment. Thus, we anticipate that improved understanding of the post-fire patterns, variations, and sources of soil carbon gleaned from this study may provide insight into the impact of fire on carbon cycling in shrub-encroached grasslands.

Materials and methods

Field site

The study site is a grass-shrub transition zone located at Sevilleta National Wildlife Refuge (SNWR) in the northern Chihuahuan Desert, New Mexico (Fig. 1). At the SNWR, the northward invasion of woody shrubs, such as creosotebush (*L. tridentata*) and mesquite (*Prosopis glandulosa* Torr.,), into perennial grasslands has been well described in the Chihuahuan Desert, attributed primarily to grassland degradation by cattle grazing and fire suppression(Báez and Collins 2008; Van Auken 2009; Puttock et al. 2014). This site is dominated by black grama and the encroachment of creosote shrubs is moderate, primarily occurring on sandy loam soil (Johnson 1988; Sankey et al. 2012a; Cunliffe et al. 2016).

The field site is a heterogeneous landscape with a mosaic of grasses (60% land coverage), shrubs (5–10%) and bare soil interspaces (30%–35%) (Dukes et al. 2018; Wang et al. 2018). The grass cover is relatively sparse at the shrub bases but provides enough connectivity to allow the spread of fire in the presence of strong winds (Ravi et al. 2009). The windy season in this area

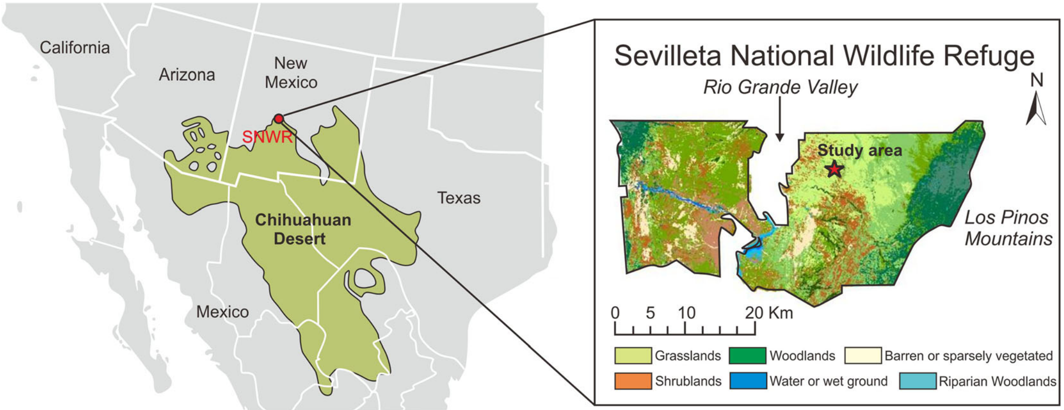

Fig. 1 Location of the study area in the Sevilleta National Wildlife Refuge (SNWR) in the northern Chihuahuan Desert, New Mexico, USA. (Data source: Sevilleta LTER)

is from March to May and the predominant wind is from the southwest (Wang et al. 2018). Annual precipitation in this area is around 250 mm and most precipitation occurs from June to September during the North American Monsoon (Báez and Collins 2008; Wang et al. 2018).

In the study area, the landscape can be subdivided into three distinct microsites, namely grass, shrub, and bare interspace. Grass microsites refer to areas with grass growth and areas beneath grass canopies. Shrub microsites are areas under shrub canopies, commonly ranging in size from 1.0 m to 2.0 m in diameter. Bare interspace microsites are characterized by soil surface with no visible vegetation coverage, which usually lie between neighboring vegetated microsites.

Experimental setup

A 100 m × 100 m monitoring area was established in March 2016 (Fig. 2). The surface condition of this area is characterized by uniform soil texture, vegetation coverage, and topography. A prescribed fire was set to burn the monitoring area on March 10, 2016, during the beginning of the windy season. The fire was ignited using hydrocarbons on the downwind edge of the experimental site, and it was restricted inside the site by a control framework around the area. The grass cover provided enough connectivity among vegetation patches to allow the spread of fire. Partially burnt shrubs were subsequently torched, ensuring complete removal of aboveground vegetation. Previous studies in the same locations indicated that fire temperatures in these systems were highly heterogeneous, with higher surface soil temperature beneath the shrubs (average 260 °C) than in grass patches (average 120 °C) and bare interspaces (< 90 °C) (Ravi et al. 2009). The monitoring area contains three 30 m × 10 m replicated plots that are oriented with the long-axis perpendicular to the predominant wind direction to minimize interactions. In the middle of each 30 m × 10 m plot, a 5 m × 5 m sampling area was established to collect soil samples (Fig. 2a).

Within each (5 m × 5 m) sampling plot, 50 randomly distributed soil samples were collected from the top 5 cm of the soil profile twice a year before and after the spring windy season. The coordinates of the sampling locations were randomly generated, and a different set of sampling locations was used for each sampling period. During the process of soil sampling, locations of the soil samples were carefully determined using a centimeter-scale coordinate system based on the axes of the 5 m × 5 m sampling area (Fig. 2a). For post-fire soil sampling, residues of the fire (e.g., ash or materials not burned completely) were carefully excluded if a soil sample was located at a grass or shrub microsite. This sampling method ensured that the existing components of soil, rather than freshly-produced charcoal and pyrogenic carbon, were collected and analyzed. The microsite type of every sampling point was also recorded. The five sampling periods were (1) Pre-burn, right before the prescribed fire in March 2016; (2) March 2016, immediately after the prescribed fire; (3) June 2016, after a windy season followed the prescribed fire; (4) March 2017, one year after the prescribed fire; and (5) June 2017, after experiencing two spring windy seasons following the prescribed fire.

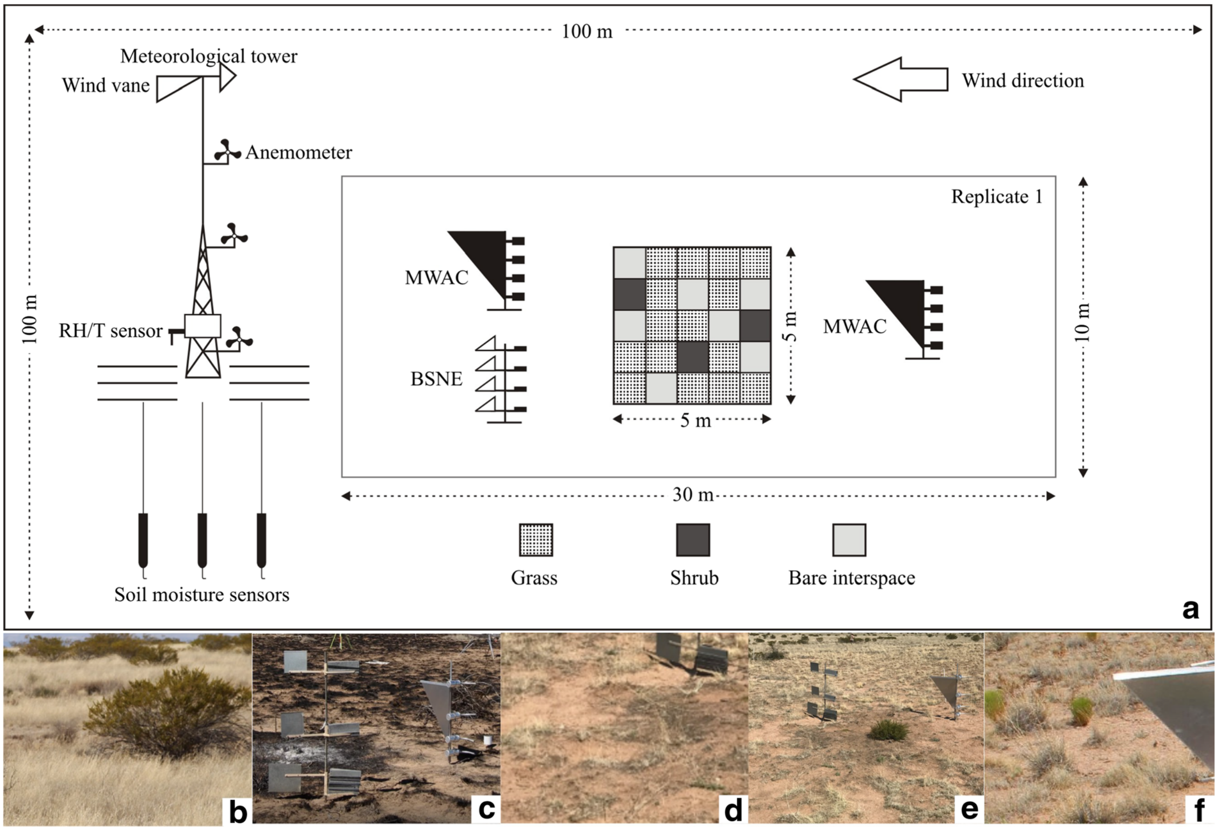

Fig. 2 *a)* Experimental layout in the field; *b)* The surface condition of the study area in Mar. 2016 before the prescribed fire; *c)* The surface condition of the burned area in Mar. 2016 immediately after the prescribed fire; *d)* The surface condition of the burned area in Jun. 2016 one spring wind season after the prescribed fire; *e)* The surface condition of the burned area in Mar. 2017; *f)* The surface condition of the burned area in Jun. 2017. Note diagram *a)* was not made to scale

A total of 31 vegetation foliar samples, representative of every visible species in the study area, were randomly collected from the monitoring area in September 2017. Names of the species, vegetation types, and conditions of the foliar samples (live, litter) were recorded. Plant cover and community composition of the treated area were monitored by four 50-m line intercept transects (parallel and perpendicular to wind direction) every March and June. A meteorological tower was also established in the monitoring area, and the recorded wind speed, precipitation, and soil water content data during the experiment period can be found in Wang et al. (2018).

Laboratory analysis

Each soil sample was passed through a 2-mm sieve to remove roots, coarse surface litter, and rock fragments (pebbles, gravels, cobbles). Soil samples were then ground to fine powder by a ball mill (PBM-04 Planetary Ball Mill, RETSCH, Germany). The inorganic carbon in each soil sample was removed by adding 2 M HCl to approximately 4 g of ground soil, left for 48 h, and then filtered and washed three times with 100 mL deionized water to remove potential $CaCl_2$ or $MgCl_2$ salts generated by acidification. Soil samples were then air-dried prior to the analysis of SOC and $\delta^{13}C$. Vegetation samples were first rinsed with deionized water, and then oven dried at 60 °C for 48 h. The vegetation samples were then ground into small pieces using a mortar and pestle. $\delta^{13}C$ in soil and vegetation samples, and SOC in soil samples were measured via flash combustion and reduction using a Thermo Finnigan Flash HT EA (high temperature elemental analyzer) coupled to a Thermo Finnigan Conflo IV and Thermo Finnigan Delta V Advantage isotope ratio mass spectrometer (IRMS).

Due to the low organic carbon content of the soil samples, approximately 15 mg of soil was required for analysis, while 2 mg of plant foliar was used. Each vegetation sample was analyzed three times and the results were averaged. Stable isotope compositions are reported in the conventional form:

$$\delta^{13}C(‰) = \left[\left({}^{13}C/{}^{12}C\right)_{sample}/\left({}^{13}C/{}^{12}C\right)_{VPDB}-1\right] \times 1000$$

where $({}^{13}C/{}^{12}C)_{sample}$ and $({}^{13}C/{}^{12}C)_{VPDB}$ are the isotopic ratios of the sample and international standard Vienna Pee Dee Belemnite (VPDB), respectively. Precision of triplicate measurements for sample $\delta^{13}C$ is 0.1‰. Reproducibility and calibration of isotope measurements are determined during each batch of samples by replicate measurements of two internal standards, plus the national standard USGS 40 (L-glutamic acid). Precision for standards is ≤0.1‰. SOC was determined by generating a carbon calibration curve by measuring an internal acetanilide standard of known carbon content prepared at several different masses.

Data analysis

For each sampling period, we calculated the mean values of SOC and $\delta^{13}C$ for the entire sampling area as well as samples associated with different microsites. The coefficient of variation of both SOC and $\delta^{13}C$ was also calculated to evaluate the overall variations among samples. One-way ANOVA was conducted to compare the mean values of SOC and $\delta^{13}C$ in different sampling periods. Two-way ANOVA was performed to identify the difference of SOC and $\delta^{13}C$ among different microsites (factor 1), and different sampling periods (factor 2). Significance of differences between two specific means were assessed with a post hoc Tukey HSD test. Unless otherwise indicated, we set $P < 0.05$ for significance. All non-geostatistical data analyses were performed using *R* software version 3.3.3 (*R* Development Core Team 2017).

The characteristics of the spatial distribution of soil SOC and $\delta^{13}C$ were quantified using geostatistical analyses. Semivariograms, which depict the average variance found in comparisons of samples taken at increasing distance from one another (Schlesinger et al. 1996), were created for SOC and soil $\delta^{13}C$ of each sampling period. A semivariogram was constructed using the lag interval of 0.2 m in each 5 m × 5 m sampling plot. The slightly larger lag interval than the minimum sample separation distance was used to better describe the potential change of soil C spatial distributions with the effect of wind erosion (Li et al. 2008). Moreover, the individual grass clumps in the study area are typically ≤20 cm in diameter, so we expected that grassland with little shrub cover would show a higher nugget value and smaller range value than grassland with more shrub cover. When comparing the isotropic and corresponding anisotropic semivariograms at 0°, 45°, 90° and 135°, we found no significant directional patterns. Therefore, isotropic semivariograms were used in all analyses.

The spherical model was used to fit the empirical SOC and soil $\delta^{13}C$ distribution (Schlesinger et al. 1996; Li et al. 2008), and three important parameters were obtained. The first parameter, range (A_0), indicates the distance of spatial autocorrelation. The second parameter, nugget (C_0), is the intercept of the *y*-axis on the semivariogram and represents variance occurred at scales finer than lag distance (Schlesinger et al. 1996). The semivariogram of the spherical model initially increases and then reaches the sill ($C_0 + C$). The third parameter, $C/(C_0 + C)$, denotes the magnitude of spatial dependence. A high $C/(C_0 + C)$ ratio suggests a strong spatial pattern, whereas a low ratio implies a random pattern (Jackson and Caldwell 1993; Schlesinger et al. 1996; Li et al. 2008, 2009a). The geostatistical analyses were conducted using the GS+ package (GS+ version 10, Gamma Design Software, Plainwell, Michigan).

Soil C source partitioning

The $\delta^{13}C$ compositions of C_3 and C_4 plants from the vegetation samples were employed in the two-source mixing ratio equation to calculate the relative percentage contributions of shrubs and grasses to SOC, following a method outlined in Wang et al. (2009):

$$\delta^{13}C_{SOC} = \delta^{13}C_{C3} \times f_{C3} + \delta^{13}C_{C4} \times f_{C4}$$

where $\delta^{13}C_{SOC}$ is the $\delta^{13}C$ value of SOC, $\delta^{13}C_{C3}$ and $\delta^{13}C_{C4}$ are the $\delta^{13}C$ values of C_3 and C_4 vegetation, respectively. The coefficients, f_{C3} and f_{C4}, which must sum to one, are relative contributions of shrubs and grasses to soil C, respectively. The end-member values of C_3 and C_4 vegetation were locally determined from the foliar $\delta^{13}C$ of grasses and shrubs at the study area (−25.2‰ for C_3 plants and − 14.3‰ for C_4 plants). Due to the limited belowground information such as root density and root distribution, the organic C source from vegetation in this study is calculated by averaging measured foliar δ^{13}C values of the vegetation type as the end-member.

Results

Soil C and δ^{13}C distributions

The overall SOC content in the surface soil (i.e., among all microsites) decreased from 0.76% to 0.61% after the fire in March 2016, and then recovered to a slightly higher level of 0.66% by June 2017 (Table 1). The change of overall SOC content, however, was not statistically significant during the experimental time period. Different from SOC, the overall soil δ^{13}C increased significantly from −19.3‰ before the fire to −17.6‰ after two windy seasons (ANOVA, $P < 0.05$, Table 1).

The coefficient of variation (CV) of both SOC and δ^{13}C among all microsites decreased substantially during the time of the experiment. Plant transect data shows that total cover, which was nonexistent immediately following the fire, recovered rapidly to 19% by June 2016 almost entirely due to re-sprouting of grasses. Total plant cover continued to increase to 26% by June 2017, still primarily due to grasses as opposed to shrubs.

For different microsites, the results show that shrub microsites had significantly higher SOC than bare interspace and grass microsites prior to and immediately following the fire, but not one year after the fire in March 2017 as well as in June 2017 (Fig. 3a). Soil δ^{13}C in shrub microsites was significantly lower than bare and grass microsites before the prescribed fire, however, this significant difference was not observed by March 2017, one year post-fire (Fig. 3b).

Both SOC and soil δ^{13}C showed strong spatial patterns before the prescribed fire, but the distance of spatial autocorrelation (A_0) for SOC was 1.91 m, which was notably larger than the 1.58 m for δ^{13}C (Fig. 4). Following the prescribed fire, the spatial autocorrelation distance for SOC increased and reached 3.74 m by June 2017 (Fig. 4). Unlike SOC, the spatial autocorrelation distance for δ^{13}C decreased during the post-fire experimental period to 0.86 m in June 2017 (Fig. 4). The prescribed fire also changed the magnitude of spatial dependence, $C/(C_0 + C)$, for SOC and δ^{13}C differently. For SOC, this parameter decreased from 98% to 81% after the prescribed fire, whereas it only changed slightly for δ^{13}C during the experimental period (Fig. 4).

Soil C partition

Overall, C_4 plants contributed a higher percentage of SOC than that of C_3 plants during the experimental period (Fig. 5). However, the relative contributions of SOC between C_4 and C_3 plants changed significantly, and C_4 plants became the dominant contributor to SOC (i.e., ~70%) two windy seasons after the prescribed fire.

For individual microsites, up to 75% of the SOC in the surface soil at bare microsites was derived from C_4 grasses, whereas the grass and shrub microsites showed more mixed SOC sources derived from C_3 and C_4 plants before the prescribed fire (Fig. 6). Fire did not appear to change the predominant contribution of C_4 plants to SOC at the bare interspaces in the study area (Fig. 6). However, the contribution of C_3 shrubs to the SOC at the shrub microsites decreased from 75% prior to the fire, to approximately 30% by June 2017 (Fig. 6). No significant changes of SOC sources were observed at the grass microsites in the study area despite the prescribed fire.

Table 1 Mean value and CV (coefficient of variation) of soil organic carbon (SOC) and soil δ^{13}C (‰), and fractional vegetation cover (plant cover %) in the study area during the experimental period

Time period	SOC		δ^{13}C		Plant cover (%)	
	Mean (%)	CV (%)	Mean (‰)	CV (%)	Shrub	Grass
Pre-burn	0.76^{a}	54.1	−19.3^{a}	−12.2	17	47
March 2016	0.61^{a}	55.6	−17.9^{b}	−11.0	0	0
June 2016	0.75^{a}	49.2	−18.6^{ab}	−13.8	1	18
March 2017	0.70^{a}	35.6	−18.2^{ab}	−10.4	3	21
June 2017	0.66^{a}	43.5	−17.6^{b}	−10.9	4	22

Note: letters indicate significant difference between two sampling times (One way ANOVA, $P < 0.05$)

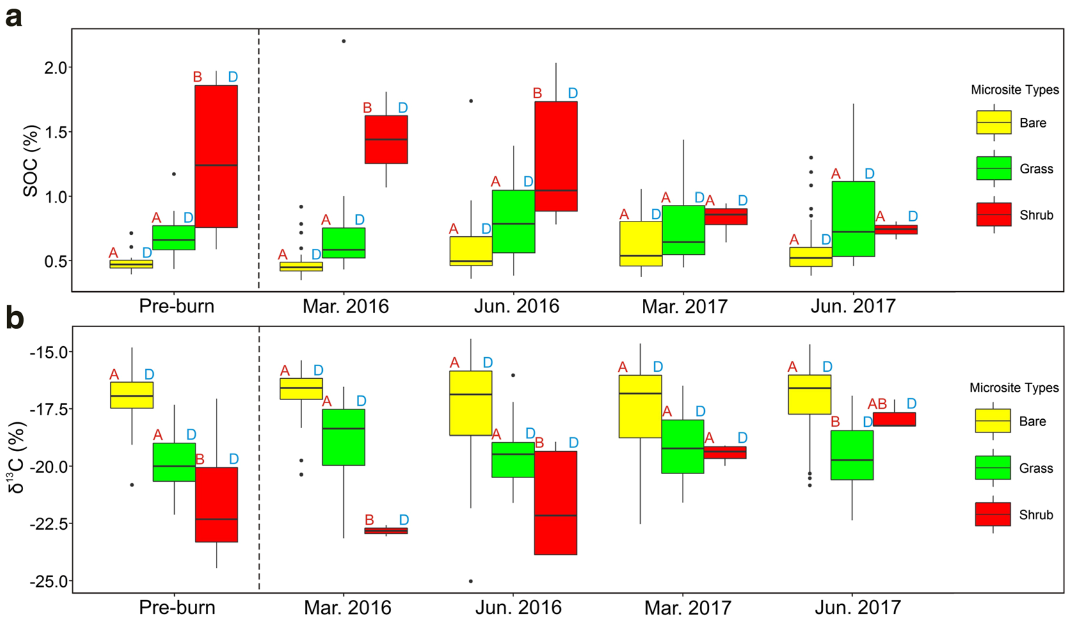

Fig. 3 The change of SOC a) and soil δ^{13}C composition b) at different microsites during the experimental time period. A two-way ANOVA was conducted for the treated area. The red letters (located on the left side of each box) show the statistical results for different microsites at each sampling time, and the blue letters (located on the right side of each box) indicate the results for the same microsite at different sampling times. Significance of difference is exhibited by different letters ($P < 0.05$). Dashed line indicates before and after the prescribed fire. Note the horizontal bars in the boxes are medians

Discussion

Post-fire changes of SOC and soil δ^{13}C

The high SOC concentration under shrubs in the study area before fire is congruent with a well-described phenomenon, islands of fertility, formed beneath shrub canopies in many arid and semiarid systems (Schelsinger et al. 1990, Schade and Hobbie 2005; Ravi et al. 2010; Field et al. 2012). The high CV and high magnitude of spatial dependence derived from geostatistical analyses for SOC and δ^{13}C suggest a heterogeneous soil C distribution before the fire, and the distance of spatial autocorrelation (1 to 2 m, Fig. 4) are consistent with the average canopy diameter of shrubs, suggesting that the SOC and δ^{13}C values of soil under a shrub canopy are similar and more closely related to each other than soil outside the canopy. These patterns are the result of the interaction of geologic, climatic, topographic, and biological variables (Legendre and Fortin 1989; Legendre 1993). Results of our study further show that, following the prescribed fire, the spatial distribution of SOC became more homogeneous, indicated by the reduced CV and declined magnitude of spatial dependence (Table 1 and Fig. 3). Along with the change in heterogeneity, the distance of spatial autocorrelation for SOC increased to well beyond the characteristic diameter of creosote bush one year after the prescribed fire. Redistribution of SOC following fire has important implications for grassland management in that it may enhance grass regrowth, thereby providing a negative feedback to woody plant encroachment and reversing associated heterogeneous surface microtopography and soil properties (D'Odorico et al. 2004; Ravi et al. 2009; Singh et al. 2012; Sankey et al. 2012a; Dukes et al. 2018).

We infer that the rapid redistribution of SOC following the fire is likely caused by enhanced wind erosion after the fire that preferentially erodes raised undershrub microsite mounds and deposits sediment in lower relief grass microsites and bare interspaces. Although we do not report on aeolian sediment transport herein, an earlier study in this treated area showed that the horizontal aeolian sediment flux was 75 g m^{-1} day^{-1}, which is nearly three times higher than the nearby undisturbed natural landscape (Dukes et al. 2018). Despite the potential increase in runoff after the fire, water-driven soil movement may be small due to the flat surface and insufficient rain events during the period of the study (Wang et al. 2018). The effects of enhanced aeolian sediment transport on the spatial distribution of SOC

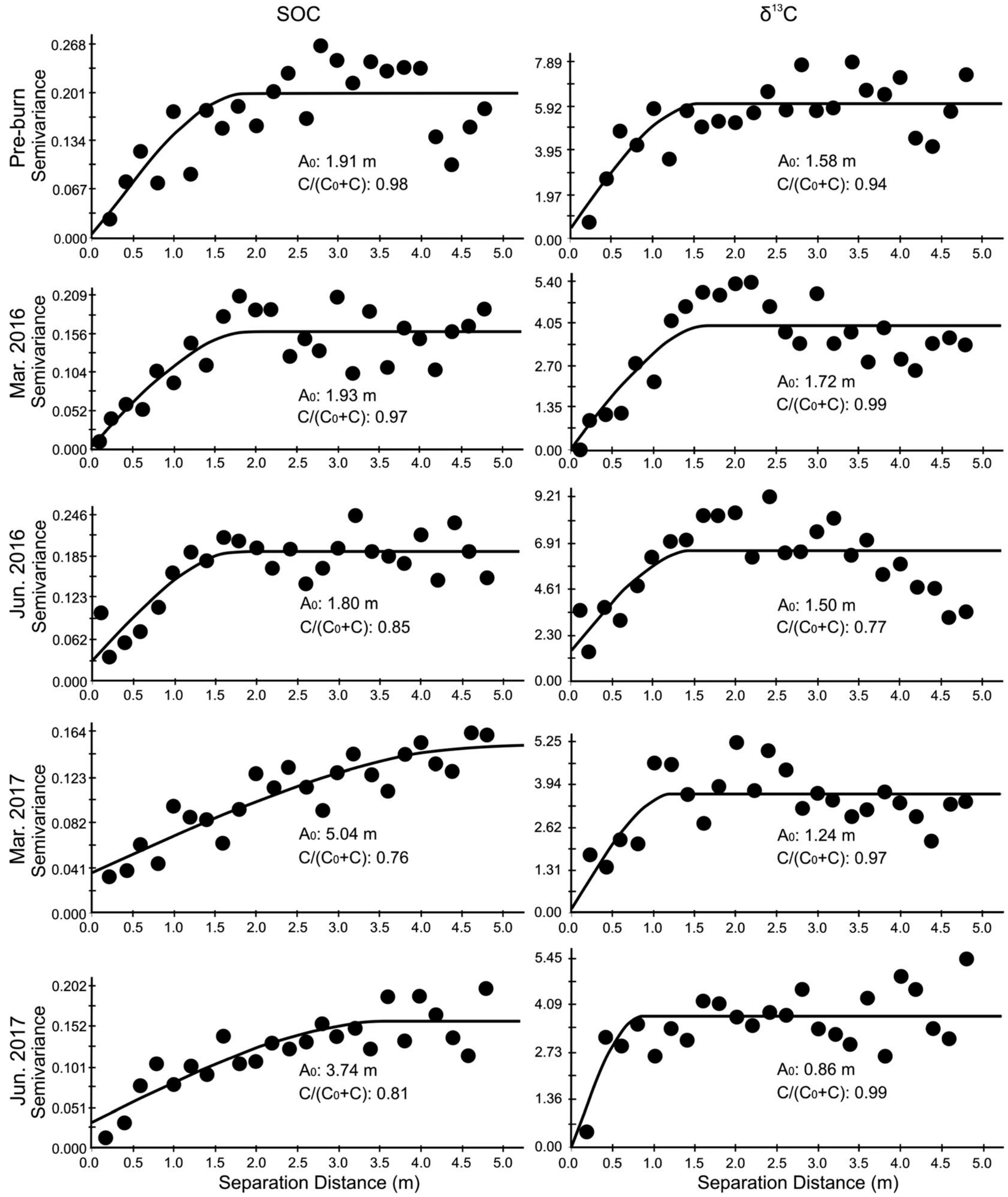

Fig. 4 Semivariograms of SOC and δ^{13}C distribution following the prescribed fire during the experiment period. Under the curve is the summary of semivariogram spherical model parameters. A_0 is the distance of spatial autocorrelation (m), and $C/(C_0 + C)$ denotes the ratio of structured variance among the samples

has also been characterized in a mesquite-encroached desert grassland at the Jornada Experimental Range, New Mexico (Li et al. 2008, 2009b), throughout the sagebrush steppe of the Great Basin, USA (Sankey et al. 2012b; Hasselquist et al. 2011), and in creosote shrublands of the Mojave Desert, USA (Kavouras et al. 2012). Biological crusts were also observed in bare interspaces, which can fix carbon and nitrogen as well as improve the stability of organic matter in bare interspaces through fire (Johansen et al. 2001; Bowker et al. 2004), therefore preventing the SOC loss in bare microsites (Fig. 3).

Deposition of ash produced by fire (e.g., Figure 2C) has been shown to stimulate C and N mineralization

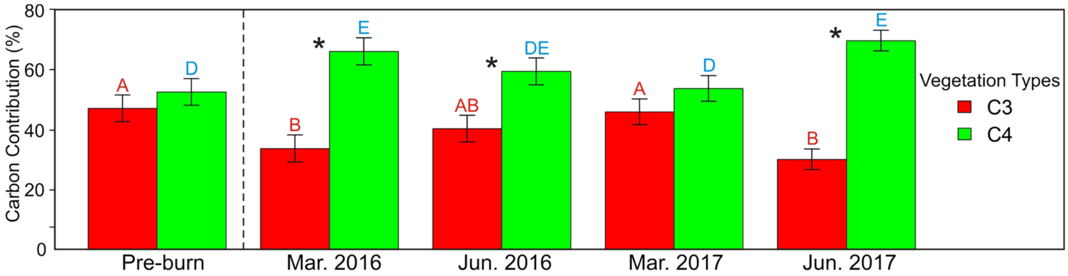

Fig. 5 The relative contributions of soil organic carbon from C_3 and C_4 plants during the experimental time period. Asterisks indicate significant difference between C_3-derived carbon and C_4-derived carbon for individual sampling periods (*t*-test, $P < 0.05$). Different letters indicate significant difference between C_3-derived carbon or C_4-derived carbon at different sampling periods (One-way ANOVA, $P < 0.05$). Dashed line indicates before and after the prescribed fire. Error bars are one standard deviation

rates (Raison 1979), leading to increased soil quality after the fire, which might help explain the rapid grass recovery rate. Visible charcoal and other pyrogenic remnants (e.g., Fig. 2C) on the soil surface just after the fire are immediately exposed to erosion processes but are highly resistant to chemical and biological alterations (Biggs et al. 2002; Czimczik et al. 2005), leading to enhanced carbon sequestration through burial (Watson et al. 1996; Preston and Schmidt 2006; De Deyn et al. 2008; Singh et al. 2012), which may partly compensate the carbon losses through atmosphere and stabilize the soil C pool after the fire.

Spatial patterns of SOC and soil $\delta^{13}C$

It is intriguing that the spatial patterns of SOC and soil $\delta^{13}C$ changed differently following the prescribed fire (Fig. 4). The different autocorrelation distances of soil $\delta^{13}C$ versus SOC may be related to differences in litter input to the soil surface beneath, on the edge, and outside of plant canopies that have been described by other studies (Throop and Archer 2008; Throop et al. 2013). For example, in comparison to C_3 shrubs, C_4 grasses-derived debris and entrained mineral materials are tightly confined to inner under-canopy areas, which are smaller than the total area affected by the C_4 grass canopy in aspects of altering wind flow and capturing wind-blown sediments. The decline of spatial autocorrelation distance and resilience of strong spatial dependence of soil $\delta^{13}C$ one year after fire may be indicative of the dependence of $\delta^{13}C$ spatial distribution on grasses, which recovered more rapidly after fire (Table 1) and tended to become the dominant nutrient sinks (Wang et al. 2018; Dukes et al. 2018). For grasses, the aboveground fibrous meristems remained after the fire, which, combined with the post-fire increased soil water content previously reported by Wang et al. (2018), helped hold the grass-derived litters within individual grass microsites. In addition, the short autocorrelation range of soil $\delta^{13}C$ post-fire (< 1.0 m) coincided with short grass-plant spacing distances and the size of grass rings previously reported by Ravi et al. (2008) in this

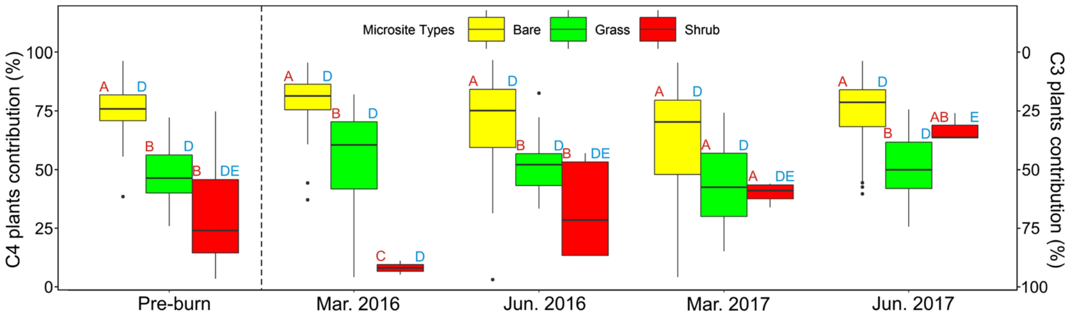

Fig. 6 The relative contribution of soil organic carbon by C_3 and C_4 plants to different microsites during the experimental time period. Red letters indicate significant difference among bare, grass and shrub microsites at individual sampling periods. Blue letters stand for significant difference for the same microsite type among the different sampling periods (Two-way ANOVA, $P < 0.05$). Dashed line indicates before and after the prescribed fire

landscape. Pyrogenic material, such as charcoal, was formed through combustion of organic material under restricted oxygen conditions. However, because the $\delta^{13}C$ value of pyrogenic carbon is controlled primarily by the $\delta^{13}C$ value of the organic material pyrolyzed (Bird and Ascough 2012), which, in this study, are C_3 or C_4 plants, we assume its appearance did not affect the soil carbon partitioning results.

Soil C sources partitioning

Results of our study highlighted a + 1.7‰ shift in soil $\delta^{13}C$ and the higher relative contributions to SOC from C_4 grasses after the fire. The initial $\delta^{13}C$ of the surface soil is determined by both abiotic factors, such as source rock, latitude, precipitation, and biotic factors, including vegetation types, decomposition, microbial activities (Bird and Pousai 1997; Klumpp et al. 2007). In our study, the prescribed fire acted as an ecological disturbance and affected the plant cover and regrowth, therefore soil $\delta^{13}C$ shows a consistent relationship with the vegetation changes. Little information is available on soil C partitioning in the desert grassland of the Chihuahuan Desert. In a dry African savanna (mean annual precipitation of 365 mm), Wang et al. (2009) reported that C_3 and C_4 vegetation contributed approximately equal amounts of overall SOC, which is similar to what we found in the pre-burn community. It is notable that crassulacean acid metabolism (CAM) plants (e.g., agave, cacti) are common in the Chihuahuan Desert and have a wide range of $\delta^{13}C$ (−11‰ to −33‰) due to their variable CO_2 uptake. However, CAM plants are not observed in our study plots and therefore isotope measurements should not reflect influence by CAM plants. Moreover, although the early stages of decomposition slightly alter the isotopic signature of plant detritus during soil organic matter formation, these changes are small relative to differences between C_3 and C_4 vegetation (~11‰) (Wedin et al. 1995; Boutton et al. 1998). Notably, the results here show that a majority of SOC was derived from C_4 grasses (i.e., >70%) two windy seasons after the prescribed fire, suggesting grasses became the major soil C source, which is in agreement with the rapid grass recovery and high grass coverage after fire (Table 1).

Our study provided further insights on the change of relative contributions of C_3 and C_4 plants to SOC at microsite scale. The higher C_4 grass contribution (>75%) at the bare interspaces is possibly due to the extensive grass root distributions, regardless of fire, at the shallow surface acting as the source for soil C. Grass microsites revealed the highest relative contribution of C_3 plants versus bare and shrub microsites two windy seasons after fire, indicating that a majority of the shrub-by litter-enriched sediments originally stored under shrub canopies were redistributed to grass microsites. The plant cover monitoring data showed that grasses recovered more rapidly compared to shrubs post-fire during the experimental time period (Table 1), suggesting grasses may have competitive advantages over shrubs after fire. The slow recovery of shrubs might be explained by a number of factors. For example, the low grazing intensity in our field site also helps grass to keep its competitive advantages against shrub longer after fires. Several studies demonstrated that seedlings of many woody shrub species are sensitive to fire (McPherson 1995; Barger et al. 2011), which, combined with limited soil moisture in shrub microsites and deceased seed dispersal due to shrub mortality, may retard shrub regrowth following fire. Eventually, the C_4-derived SOC increased at the shrub microsites, whereas the proportion of C_3-derived SOC increased at both bare and grass microsites after the prescribed fire. These observations suggest that preferred (predominant) pathway(s) of SOC movement may exist following fire. The selective movement of soil material among microsites in the study area has been confirmed by a recent study, which, by using a tracer-based approach, demonstrated that significant post-fire movement of sediment from shrub-to-grass, but not grass-to-shrub microsites, occurred (Dukes et al. 2018).

Implication for future SOC change

Climate projections suggest that the southwestern United States may experience increased temperature, decreased or more variable precipitation, and severe droughts in the near future (Seager et al. 2007, 2013; Udall and Overpeck 2017). As a result, the frequency and intensity of wildfires are expected to increase substantially (Westerling et al. 2006; Bowman et al. 2009; Sankey et al. 2017). Such changes in fire regime are anticipated to increase soil erosion by wind and water, and potentially prolong the post-fire windows of time during which increased soil erosion occurs (Hurtt et al. 2002; Field et al. 2010; Barger et al. 2011; Sankey et al. 2017; Dukes et al. 2018). Thus, land management plans need to be carefully considered to adapt to potential fire regime changes in the area. Additionally, grassland to shrubland conversion may be facilitated by wetter winters and drier summers, whereas the higher water-use efficiency of C_4 grasses may allow grasses to survive through long-term droughts (Sperry and Hacke 2002; Gao and Reynolds 2003; Parmesan and Galbraith 2004). While our study focused on the post-fire redistribution of sources of SOC at the soil surface, future studies using soil depth profiles may provide more comprehensive information on SOC partitioning to reconstruct the historic effects of the woody shrub encroachment on soil resources, and to predict future soil development in the context of climate change.

Conclusions

Results of our study highlight the role of fire in changing the spatial distributions of SOC and soil $\delta^{13}C$ in a grassland-shrubland transition zone. Interestingly, the changes in the spatial patterns of SOC and soil $\delta^{13}C$ differed following the fire. The spatial autocorrelation distance for SOC increased post-fire, probably due to the removal of shrubs by fire and subsequent soil erosion. The range of autocorrelation for $\delta^{13}C$ decreased post-fire, and the contribution of SOC from C_4 grasses compared to C_3 shrubs increased, which we infer were due to the more rapid recovery of grasses after the fire. In contrast to changes observed for shrub microsites, C derived from C_4 grasses was the dominant source of SOC at bare soil interspaces both pre and post-fire. Thus, our SOC and $\delta^{13}C$ analyses enabled the reconstruction of post-fire organic carbon inputs to soil at high spatial resolution of individual soil microsites and suggest that SOC may have moved among different microsites following the fire via pathways that can be predicted by soil erosion and deposition dynamics. Overall, changes in the spatial distribution of SOC and relative contributions of $\delta^{13}C$ that we observed, provide new insights that fire can have profound impacts on soil carbon pools during the process of shrub encroachment.

Acknowledgements This research was supported by the U.S. National Science Foundation Award EAR-1451489 for J. Li, EAR-1451518 for S. Ravi, and the Sevilleta LTER Summer Research Fellowship for G. Wang. The authors greatly acknowledge Jon Erz, Eric Krueger and Andy Lopez (FWS, SNWR), Scott Collins and Amaris Swan (Sevilleta LTER, New Mexico), and Julie McDonald (The University of Tulsa) for their assistance in field work and laboratory analysis. This manuscript is submitted for publication with the understanding that the US Government is authorized to reproduce and distribute reprints for Governmental purposes. Any use of trade, firm, or product names is for descriptive purposes only and does not imply endorsement by the U.S. Government. The data used in the paper can be accessed at http://sev.lternet.edu/ (DOI: doi:https://doi.org/10.6073/pasta/993cd7029af115ee4508c2a688af7bf9).

References

Archer SR, Andersen EM, Predick KI, Schwinning S, Steidl RJ, Woods SR (2017) Woody plant encroachment: causes and consequences. In Rangeland Systems (pp. 25-84). Springer, Cham

Báez S, Collins SL (2008) Shrub invasion decreases diversity and alters community stability in northern Chihuahuan Desert plant communities. PLoS One 3(6):e2332

Bai E, Boutton TW, Wu XB, Liu F, Archer SR (2009) Landscape-scale vegetation dynamics inferred from spatial patterns of soil $\delta^{13}C$ in a subtropical savanna parkland. Journal of Geophysical Research: Biogeosciences 114(G1)

Barger NN, Archer SR, Campbell JL, Huang CY, Morton JA, Knapp AK (2011) Woody plant proliferation in north American drylands: a synthesis of impacts on ecosystem carbon balance. Journal of Geophysical Research: Biogeosciences 116(G4)

Bender MM (1968) Mass spectrometric studies of carbon 13 variations in corn and other grasses. Radiocarbon 10(2): 468–472

Biggs TH, Quade J, Webb RH (2002) $\delta^{13}C$ values of soil organic matter in semiarid grassland with mesquite (Prosopis) encroachment in southeastern Arizona. Geoderma 110(1–2): 109–130

Bird MI, Ascough PL (2012) Isotopes in pyrogenic carbon: a review. Org Geochem 42(12):1529–1539

Bird MI, Pousai P (1997) Variations of δ13C in the surface soil organic carbon pool. Glob Biogeochem Cycles 11(3):313–322

Bird SB, Herrick JE, Wander MM, Wright SF (2002) Spatial heterogeneity of aggregate stability and soil carbon in semi-arid rangeland. Environ Pollut 116(3):445–455

Bond WJ, Stock WD, Hoffman MT (1994) Has the Karoo spread? A test for desertification using carbon isotopes from soils. S Afr J Sci 90(7):391–397

Boutton TW, Archer SR, Midwood AJ, Zitzer SF, Bol R (1998) $\delta^{13}C$ values of soil organic carbon and their use in documenting vegetation change in a subtropical savanna ecosystem. Geoderma 82(1–3):5–41

Bowker MA, Belnap J, Rosentreter R, Graham B (2004) Wildfire-resistant biological soil crusts and fire-induced loss of soil stability in Palouse prairies, USA. Appl Soil Ecol 26(1):41–52

Bowman DM, Balch JK, Artaxo P, Bond WJ, Carlson JM, Cochrane MA, D'Antonio CM, DeFries RS, Doyle JC, Harrison SP, Johnston FH (2009) Fire in the earth system. Science 324(5926):481–484

Campbell A, Miles L, Lysenko I, Hughes A, Gibbs H (2008) Carbon storage in protected areas: technical report. The United Nations environment Programme world conservation monitoring Centre. UK, Cambridge

Cunliffe AM, Puttock AK, Turnbull L, Wainwright J, Brazier RE (2016) Dryland, calcareous soils store (and lose) significant quantities of near-surface organic carbon. Journal of Geophysical Research: Earth Surface 121(4):684–702

Czimczik CI, Schmidt MWI, Schulze ED (2005) Effects of increasing fire frequency on black carbon and organic matter in Podzols of Siberian scots pine forests. Eur J Soil Sci 56(3): 417–428

D'Odorico P, Porporato A, Laio F, Ridolfi L, Rodriguez-Iturbe I (2004) Probabilistic modeling of nitrogen and carbon dynamics in water-limited ecosystems. Ecol Model 179(2):205–219

De Deyn GB, Cornelissen JH, Bardgett RD (2008) Plant functional traits and soil carbon sequestration in contrasting biomes. Ecol Lett 11(5):516–531

Deines P (1980) The isotopic composition of reduced organic carbon. In: Fritz P, Fontes JC (eds) Handbook of environmental isotope geochemistry; volume 1, the terrestrial environment, a, vol 1. Elsevier, Amsterdam, pp 329–406

Development Core Team R (2017) R: a language and environment for statistical computing. In: R Foundation for statistical computing. Austria. URL, Vienna http://www.R-project.org/

D'Odorico P, Okin GS, Bestelmeyer BT (2012) A synthetic review of feedbacks and drivers of shrub encroachment in arid grasslands. Ecohydrology 5(5):520–530

Dukes D, Gonzales HB, Ravi S, Grandstaff DE, Van Pelt RS, Li J, Wang G, Sankey JB (2018) Quantifying post-fire Aeolian sediment transport using rare earth element tracers. Journal of Geophysical Research: Biogeosciences 123:288–299

Eswaran H, Reich PF, Kimble JM, Beinroth FH, Padmanabhan E, Moncharoen P (2000) Global carbon sinks. In: Global Climate Change, Press PCCRC (eds) Lal, R., Kimble, J.M., Eswaran, H., Stewart, B.A. USA, Boca Raton, FL

Farquhar GD, Hubick KT, Condon AG, Richards RA (1989) Carbon isotope fractionation and plant water-use efficiency. In: Stable isotopes in ecological research. Springer, New York, NY, pp 21–40

Field JP, Belnap J, Breshears DD, Neff JC, Okin GS, Whicker JJ, Painter TH, Ravi S, Reheis MC, Reynolds RL (2010) The ecology of dust. Front Ecol Environ 8(8):423–430

Field JP, Breshears DD, Whicker JJ, Zou CB (2012) Sediment capture by vegetation patches: implications for desertification and increased resource redistribution. Journal of Geophysical Research: Biogeosciences 117(G1)

Gao Q, Reynolds JF (2003) Historical shrub–grass transitions in the northern Chihuahuan Desert: modeling the effects of shifting rainfall seasonality and event size over a landscape gradient. Glob Chang Biol 9(10):1475–1493

Hasselquist NJ, Germino MJ, Sankey JB, Ingram LJ, Glenn NF (2011) Aeolian nutrient fluxes following wildfire in sagebrush steppe: implications for soil carbon storage. Biogeosciences 8(12):3649–3659

Hurtt GC, Pacala SW, Moorcroft PR, Caspersen J, Shevliakova E, Houghton RA, Moore BIII (2002) Projecting the future of the US carbon sink. Proc Natl Acad Sci 99(3):1389–1394

Jackson RB, Caldwell MM (1993) Geostatistical patterns of soil heterogeneity around individual perennial plants. J Ecol 81: 683–692

Jackson RB, Banner JL, Jobbágy EG, Pockman WT, Wall DH (2002) Ecosystem carbon loss with woody plant invasion of grasslands. Nature 418(6898):623–626

Johansen MP, Hakonson TE, Breshears DD (2001) Post-fire runoff and erosion from rainfall simulation: contrasting forests with shrublands and grasslands. Hydrol Process 15(15): 2953–2965

Johnson, W. R. (1988). Soil survey of Socorro county area, New Mexico

Kavouras IG, Nikolich G, Etyemezian V, DuBois DW, King J, Shafer D (2012) In situ observations of soil minerals and organic matter in the early phases of prescribed fires. Journal of Geophysical Research: Atmospheres 117(D12)

Klumpp K, Soussana JF, Falcimagne R (2007) Long-term steady state 13 C labelling to investigate soil carbon turnover in grasslands. Biogeosciences 4(3):385–394

Legendre P (1993) Spatial autocorrelation: trouble or new paradigm? Ecology 74(6):1659–1673

Legendre P, Fortin MJ (1989) Spatial pattern and ecological analysis. Vegetatio 80(2):107–138

Li J, Okin GS, Alvarez L, Epstein H (2008) Effects of wind erosion on the spatial heterogeneity of soil nutrients in two desert grassland communities. Biogeochemistry 88(1):73–88

Li J, Okin GS, Alvarez LJ, Epstein HE (2009a) Sediment deposition and soil nutrient heterogeneity in two desert grassland ecosystems. southern New Mexico Plant and soil 319(1–2): 67–84

Li J, Okin GS, Epstein HE (2009b) Effects of enhanced wind erosion on surface soil texture and characteristics of windblown sediments. Journal of Geophysical Research: Biogeosciences 114(G2)

McPherson GR (1995) The role of fire in desert grasslands. The desert grassland:130–151

Minckley TA, Long CJ (2016) Paleofire severity and vegetation change in the Cascade Range, Oregon. USA Quaternary Research 85(2):211–217

Parmesan C, Galbraith H (2004) Observed impacts of global climate change in the US, vol 12. Pew Center on Global Climate Change, Arlington, VA, USA

Petrie MD, Collins SL, Swann AM, Ford PL, Litvak ME (2015) Grassland to shrubland state transitions enhance carbon sequestration in the northern Chihuahuan Desert. Glob Chang Biol 21(3):1226–1235

Plaza-Bonilla D, Arrúe JL, Cantero-Martínez C, Fanlo R, Iglesias A, Álvaro-Fuentes J (2015) Carbon management in dryland agricultural systems. A review Agronomy for sustainable development 35(4):1319–1334

Preston CM, Schmidt MWI (2006) Black (pyrogenic) carbon: a synthesis of current knowledge and uncertainties with special consideration of boreal regions. Biogeosciences 3:397–420

Puttock A, Dungait JA, Macleod CJ, Bol R, Brazier RE (2014) Woody plant encroachment into grasslands leads to accelerated erosion of previously stable organic carbon from dryland soils. Journal of Geophysical Research: Biogeosciences 119(12):2345–2357

Raison RJ (1979) Modification of the soil environment by vegetation fires, with particular reference to nitrogen transformations: a review. Plant Soil 51(1):73–108

Ravi S, D'Odorico P, Wang L, Collins S (2008) Form and function of grass ring patterns in arid grasslands: the role of abiotic controls. Oecologia 158(3):545–555

Ravi S, D'Odorico P, Wang L, White CS, Okin GS, Macko SA, Collins SL (2009) Post-fire resource redistribution in desert grasslands: a possible negative feedback on land degradation. Ecosystems 12(3):434–444

Ravi S, Breshears DD, Huxman TE, D'Odorico P (2010) Land degradation in drylands: interactions among hydrologic–aeolian erosion and vegetation dynamics. Geomorphology 116(3–4):236–245

Sankey JB, Ravi S, Wallace CS, Webb RH, Huxman TE (2012a) Quantifying soil surface change in degraded drylands: shrub encroachment and effects of fire and vegetation removal in a desert grassland. Journal of Geophysical Research: Biogeosciences 117(G2)

Sankey JB, Germino MJ, Sankey TT, Hoover AN (2012b) Fire effects on the spatial patterning of soil properties in sagebrush steppe, USA: a meta-analysis. Int J Wildland Fire 21(5):545–556

Sankey JB, Kreitler J, Hawbaker TJ, McVay JL, Miller ME, Mueller ER, Vaillant NM, Lowe SE, Sankey TT (2017) Climate, wildfire, and erosion ensemble foretells more sediment in western USA watersheds. Geophys Res Lett 120(4):349

Sarukhan, J., Whyte, A., Hassan, R., Scholes, R., Ash, N., Carpenter, S.T., Pingali, P.L., Bennett, E.M., Zurek, M.B., Chopra, K., Leemans, R. (2005). Millenium ecosystem assessment: ecosystems and human well-being

Schade JD, Hobbie SE (2005) Spatial and temporal variation in islands of fertility in the Sonoran Desert. Biogeochemistry 73(3):541–553

Schlesinger WH, Reynolds JF, Cunningham GL, Huenneke LF, Jarrell WM, Virginia RA, Whitford WG (1990) Biological feedbacks in global desertification. Science 247(4946):1043–1048

Schlesinger WH, Raikes JA, Hartley AE, Cross AF (1996) On the spatial pattern of soil nutrients in desert ecosystems. Ecology 77(2):364–374

Seager R, Ting M, Held I, Kushnir Y, Lu J, Vecchi G, Huang HP, Harnik N, Leetmaa A, Lau NC, Li C (2007) Model projections of an imminent transition to a more arid climate in southwestern North America. Science 316(5828):1181–1184

Seager R, Ting M, Li C, Naik N, Cook B, Nakamura J, Liu H (2013) Projections of declining surface-water availability for the southwestern United States. Nat Clim Chang 3(5):482–486

Singh N, Abiven S, Torn MS, Schmidt MWI (2012) Fire-derived organic carbon in soil turns over on a centennial scale. Biogeosciences 9(8):2847–2857

Smith BN, Epstein S (1971) Two categories of $^{13}C/^{12}C$ ratios for higher plants. Plant Physiol 47(3):380–384

Sperry JS, Hacke UG (2002) Desert shrub water relations with respect to soil characteristics and plant functional type. Funct Ecol 16(3):367–378

Throop HL, Archer SR (2008) Shrub (Prosopis velutina) encroachment in a semidesert grassland: spatial–temporal changes in soil organic carbon and nitrogen pools. Glob Chang Biol 14(10):2420–2431

Throop HL, Lajtha K, Kramer M (2013) Density fractionation and ^{13}C reveal changes in soil carbon following woody encroachment in a desert ecosystem. Biogeochemistry 112(1–3):409–422

Turnbull L, Wilcox BP, Belnap J, Ravi S, D'odorico P, Childers D, Gwenzi W, Okin G, Wainwright J, Caylor KK, Sankey T (2012) Understanding the role of ecohydrological feedbacks in ecosystem state change in drylands. Ecohydrology 5(2):174–183

Udall B, Overpeck J (2017) The twenty-first century Colorado River hot drought and implications for the future. Water Resour Res 53(3):2404–2418

Van Auken OW (2009) Causes and consequences of woody plant encroachment into western north American grasslands. J Environ Manag 90(10):2931–2942

Wang L, Okin GS, Caylor KK, Macko SA (2009) Spatial heterogeneity and sources of soil carbon in southern African savannas. Geoderma 149(3–4):402–408

Wang G, Li J, Ravi S, Dukes D, Gonzales HB, Sankey JB (2018) Post-fire redistribution of soil carbon and nitrogen at a grassland–Shrubland ecotone. Ecosystems:1–15

Watson RT, Zinyowera MC, Moss RH (1996) Climate change 1995. Impacts. In: Adaptations and mitigation of climate change: scientific-technical analyses. Cambridge University Press, Cambridge

Wedin DA, Tieszen LL, Dewey B, Pastor J (1995) Carbon isotope dynamics during grass decomposition and soil organic matter formation. Ecology 76(5):1383–1392

West JB, Bowen GJ, Cerling TE, Ehleringer JR (2006) Stable isotopes as one of nature's ecological recorders. Trends Ecol Evol 21(7):408–414

Westerling AL, Hidalgo HG, Cayan DR, Swetnam TW (2006) Warming and earlier spring increase western US forest wildfire activity. Science 313(5789):940–943